HHS Public Access

Author manuscript

Clin Cancer Res. Author manuscript; available in PMC 2017 February 01.

Published in final edited form as:

Clin Cancer Res. 2016 February 1; 22(3): 621–632. doi:10.1158/1078-0432.CCR-15-0114.

Modulation of glucocorticoid resistance in pediatric T-cell Acute Lymphoblastic Leukemia by increasing BIM expression with the PI3K/mTOR inhibitor BEZ235

Connor P. Hall[1,2], **C. Patrick Reynolds**[1,3,4,5], and **Min H. Kang**[1,2,3,5]

[1]Cancer Center, School of Medicine, Texas Tech University Health Sciences Center, Lubbock, TX

[2]Pharmacology and Neuroscience, School of Medicine, Texas Tech University Health Sciences Center, Lubbock, TX

[3]Cell Biology & Biochemistry, School of Medicine, Texas Tech University Health Sciences Center, Lubbock, TX

[4]Pediatrics, School of Medicine, Texas Tech University Health Sciences Center, Lubbock, TX

[5]Internal Medicine, School of Medicine, Texas Tech University Health Sciences Center, Lubbock, TX

Abstract

Purpose—The aim of our study is to evaluate the preclinical therapeutic activity and mechanism of action of BEZ235, a dual PI3K/mTOR inhibitor, in combination with dexamethasone in ALL.

Experimental Design—The cytotoxic effects of BEZ235 and dexamethasone as single agents and in combination were assessed in a panel of ALL cell lines and xenograft models. The underlying mechanism of BEZ235 and dexamethasone was evaluated using immunoblotting, TaqMan RT-PCR, siRNA, immunohistochemistry and immunoprecipitation.

Results—Inhibition of the PI3K/AKT/mTOR pathway with the dual PI3K/mTOR inhibitor BEZ235 enhanced dexamethasone-induced anti-leukemic activity in *in vitro* (continuous cell lines and primary ALL cultures) and systemic *in vivo* models of T-ALL (including a patient-derived xenograft). Through inhibition of AKT1, BEZ235 was able to alleviate AKT1-mediated suppression of dexamethasone-induced apoptotic pathways leading to increased expression of the pro-apoptotic BCL-2 protein BIM. Downregulation of MCL-1 by BEZ235 further contributed to the modulation of dexamethasone resistance by increasing the amount of BIM available to induce

Correspondence: Min H. Kang, PharmD, Cell Biology & Biochemistry, School of Medicine, Texas Tech University Health Sciences Center, 3601 4th Street STOP 9445, Lubbock, TX 79430, Phone: 806-743-2694; Fax: 806-743-2990, min.kang@ttuhsc.edu.

Conflicts of Interest: The authors declare no conflict of interest.

Author Contribution

CH, CPR, and MK were involved in the research design, analysis of results, and writing the manuscript. CH performed all experiments. All authors approved the final version of this manuscript.

Disclosure: This work was funded by an R15 grant from the National Institute of Health (NIH) to MK (1R15CA159308-01). BEZ235 was kindly provided by Novartis Pharmaceuticals.

apoptosis, especially in PTEN-null T-ALL where inhibition of AKT only partially overcame AKT-induced BIM suppression.

Conclusion—Our data support the further investigation of agents targeting the PI3K/mTOR pathway to modulate glucocorticoid resistance in T-ALL.

Keywords

BEZ235; Dexamethasone; acute lymphoblastic leukemia; AKT; BIM; MCL-1

Introduction

Glucocorticoids (GCs) represent an important component of pediatric Acute Lymphoblastic Leukemia/Lymphoma (ALL) treatment. By themselves, GCs can achieve clinical remission in ALL, and with the addition of other chemotherapeutic agents, contribute to over eighty percent of patients achieving long-term event-free and overall survival (1, 2). Additionally, early response to GCs is a positive prognostic indicator and those patients who lack a robust response more frequently experience negative outcomes (3–5). Therefore, investigating the mechanisms leading to GC resistance may identify biomarkers and targets that potentially improve overall outcomes.

Inappropriate activation of the oncogenic phosphatidylinositol 3-kinase (PI3K)- AKT, mammalian target of rapamycin (mTOR) signaling pathway (PI3K/AKT/mTOR pathway) contributes to the pathogenesis and chemotherapy resistance observed in many cancers, including hematological malignancies (6–8). Activation of the PI3K/AKT/mTOR pathway in ALL depends on a large number of mechanisms including deletion/inactivation of the phosphatase and tensin homologue (PTEN), SH2 domain-containing inositol phosphatase 1 (SHIP1) inactivation, and mutations in PI3K, AKT, RAS, NOTCH1, or receptor tyrosine kinases (RTKs) (9–12). In both higher risk B-cell (B-ALL) and more notably T-cell ALL (T-ALL) primary bone marrow samples, AKT hyperactivation has been observed (12, 13). In one study of T-ALL, eighty-five percent of primary patient samples were characterized by increased AKT phosphorylation when compared with normal thymocyte controls (12). Consequently, this AKT hyperactivation has been correlated with reduced responses to induction therapy and poor overall and relapse-free survival (13). Two frequent mutations associated with increased AKT activity in T-ALL occur in *NOTCH1*, which is represented in greater than 50% of all T-ALL (14), and *PTEN*, which is estimated to be present in 8 to 30% of all T-ALL (9, 10, 15, 16). Interestingly, *NOTCH1* activating mutations can downregulate *PTEN* via HES1 (15), suggesting PTEN dysfunction is an important biological characteristic of T-ALL. Reduced PTEN activity leads to increased PI3K/AKT pathway activity and has also been associated with poor outcomes (9, 10, 12, 16). PTEN is a negative regulator of the PI3K/AKT/mTOR pathway by dephosphorylating phosphatidylinositol-3,4,5-triphosphate (PIP_3) to phosphatidylinositol-4,5-biphosphate (PIP_2) counteracting the action of PI3K and eliminating AKT recruitment to the cell membrane where it is phosphorylated by phosphoinositide-dependent protein kinase (PDK1) at Thr308 and by mTORC2 at Ser473 to become activated (17). Activated AKT phosphorylates over 100 different substrates ultimately promoting increased cell survival, proliferation, growth, protein synthesis, and metabolism (8, 17, 18).

As constitutive activation of the PI3K/AKT/mTOR pathway occurs so frequently in T-ALL and is associated with treatment resistance, this makes it an attractive target to improve treatment responses in this disease. We and others previously demonstrated that rapamycin enhanced dexamethasone activity in *in vitro* and *in vivo* models of T-ALL (19, 20). Despite the promising activity seen with the latter combination, the immunosuppressive effects of rapamycin in combination with dexamethasone was concerning and therefore not pursued further (20). Over the last decade, various targeted inhibitors of the PI3K/AKT/mTOR pathway have been developed. The first to enter clinical trials was BEZ235, a dual PI3K/mTOR inhibitor which is currently on hold in development due to low oral bioavailability after Phase I/II clinical trials in adults with solid and hematological malignancies as a single agent and in combination (21–25). As a single agent, BEZ235 was well-tolerated in adult leukemia patients (21), providing a possible alternative to rapamycin. In this study, we show that BEZ235 increased dexamethasone-induced apoptosis through increasing BIM in T-ALL models. This activity is due to BEZ235 inhibition of AKT1, which is a crucial mediator suppressing BIM expression in response to dexamethasone. We also show that BEZ decreases MCL-1 through a mechanism distinctive from AKT inactivation. The decrease in MCL-1 by BEZ235 may represent importance in T-ALL with *PTEN* mutation/deletion, suggesting that the targeting of multiple kinases in this pathway will be critical to reverse GC resistance in pediatric patients with T-ALL.

Methods

In vitro cell lines and culture

Human pediatric T-ALL cell lines established from children at diagnosis (COG-LL-329h) and relapse (COG-LL-317h, COG-LL-332h) and B-ALL cell lines established at diagnosis (COG-LL-319h, COG-LL-402h) and relapse (COG-LL-355h) were provided by the Children's Oncology Group (COG) Cell Line and Xenograft Repository (www.cogcell.org). Human T-ALL cell line TX-LY-172h (established from a child at relapse) was obtained from the Texas Cancer Cell Repository (TXCCR, www.txccr.org). COG and TXCCR cell lines were cultured in Iscove's Modified Dulbecco medium (IMDM; Thermo-Scientific, Waltham. MA) supplemented with 3mM L-glutamine, 5μg/mL insulin, and 20% heat-inactivated fetal bovine serum (FBS). Nalm-6 (pre-B ALL, obtained from Deutsche Sammlung von Mikroorganismem und Zellkulturen (DSMZ), German Collection of Microorganisms and Cell Cultures, Braunschweig, Germany), and RS4;11 (pre-B ALL), T-ALL cell lines (CCRF-CEM, MOLT-3, and MOLT-4) from American Type Culture Collection (ATCC, Manassas, VA) were cultured in RPMI-1640 medium (Thermo-Scientific, Waltham, MA) supplemented with 10% heat-inactivated FBS. All cell lines were maintained and treated with drugs in a 37°C incubator with 5% O_2 (bone marrow-level hypoxia), 5% CO_2, and 90% N_2. Karyotype information of the cell lines is included in Supplementary Table 1. Cell line identities were confirmed after each expansion and prior to freezing by short tandem repeat (STR) profiling. Profiles for each cell line were unique except for pairs of cell lines established from the same patient at different stages of the disease (COG-LL-329h and COG-LL-332h, MOLT-3 and MOLT-4), and were verified in the COG cell line + Xenograft STR database (www.COGcell.org). All cultures were confirmed to be free of mycoplasma and epstein-barr virus (EBV) contamination. Studies

using tissues from human subjects were approved by the Institutional Review Board (IRB) of Texas Tech University Health Sciences Center.

Primary Cells

Clinical specimens were obtained with consent via a biobanking protocol approved by the TTUHSC committee for protection of human subjects. Ficoll separated mononuclear cells from peripheral blood of pediatric patients diagnosed with ALL (obtained with informed consent under COG biobanking protocol ABTR04B1) were obtained from Children's Oncology Group (COG; www.cogcell.org) or the Texas Cancer Cell Repository (TXCCR; www.txccr.org). All patients gave informed consent; the study using the primary samples was approved by the TTUHSC Institutional Review Board. Mononuclear cells were verified to contain >80% leukemic blasts by flow cytometry using CD45 and CD7 for T-ALL samples or CD45 and CD19 for B-ALL samples. Isolated cells were cultured over a layer of immortalized HS-5 human bone marrow stromal cells (American Type Culture Collection [ATCC], Manassas, VA, USA) in Iscove's Modified Dulbecco medium (IMDM; Thermo-Scientific, Waltham, MA, USA) supplemented with 3mM L-glutamine, 5μg/mL insulin, 20% heat-inactivated fetal bovine serum (FBS), recombinant IL-7 (10ng/mL; R&D Systems, Minneapolis, MN, USA), recombinant stem cell factor (50ng/mL; R&D Systems), and recombinant Flt-3 ligand (20ng/mL; R&D Systems). All primary cells were maintained and treated with drugs in a 37°C incubator with 5% O_2 (bone marrow-level hypoxia) (26, 27), 5% CO_2, and 90% N_2. Cytotoxicity experiments were performed in 24 well plates. Viability of the cells was assessed by flow cytometry after staining with the FITC Annexin V Apoptosis Detection Kit (BD Biosciences, San Jose, CA, USA) following manufacturer's protocol. Viability was calculated as the percent of cells not staining for Annexin V or Propidium Iodide.

Cytotoxicity, Apoptosis and Cell Cycle Assays

The *in vitro* cytotoxic activities of dexamethasone, BEZ235, and the BEZ235 plus dexamethasone combination were determined using the DIMSCAN digital imaging microscopy cytotoxicity system as described previously (28). One day prior to drug addition, cells were seeded in 96 well plates at a density previously determined to result in confluence in non-treated wells. Cells were exposed to DMSO, BEZ235, dexamethasone, or BEZ235 plus dexamethasone for a total of 48 to 96 hours before addition of fluorescein diacetate (FDA) and eosin Y. Fluorescence was measured in each well and quantified by DIMSCAN software. To detect apoptosis, treated cells were harvested and stained using the FITC Annexin V Apoptosis Detection Kit I (BD Biosciences) following manufacturer's protocol. Cell cycle analysis was performed using a propidium iodide staining protocol as described previously (29).

Immunohistochemistry

Sections (4 μm) from formalin-fixed, paraffin-embedded spleens were processed for immunohistochemistry and stained with hematoxylin and eosin. BIM was detected using BIM antibody (Cell Signaling, Danvers, MA) and the VECTASTAIN ABC Kit for Rabbit IgG (Vector Laboratories, Burlingame, CA) according to manufacturer's instructions. The

sections were examined using a light microscope (BX51; Olympus, Tokyo, Japan). Images were capture using CellSens® Standard 1.6 (Olympus, Tokyo, Japan).

RNA interference

ON-TARGETplus *AKT1* SmartPool siRNA and ON-TARGETplus Non-Targeting Control Pool were purchased from Thermo-Scientific. *BCL2L11* Silencer Select siRNA and *MCL1* Silencer Select siRNA were purchased from Life Technologies (Carlsbad, CA, USA). Transfections were performed using the Nucleofector 4D system (Lonza Biologics, Hopkinton, MA, USA) with conditions optimized for the respective cell lines (Solution SF; Program CM-137; 1μM siRNA). Three million COG-LL-317h or RS4;11 cells were used per transfection. Following transfection, cells were plated and incubated for 16 hours before experiments.

In vivo experiments

Mice were housed in specific pathogen-free animal facilities located at Texas Tech University Health Sciences Center and all mouse procedures were in accordance with the guidelines of Texas Tech University Health Sciences Center Institutional Animal Care and Use Committee. For bioluminescent models, 2×10^6 COG-LL-317h expressing the luciferase gene (pCCL-c-MNDU3c-LUC-PGK-hB7 vector using human B7.1 (CD80) as a selection marker) and sorted to greater than 90% CD80 positivity were injected intravenously via tail vein into female non-obese diabetic (NOD)/severe-combined immunodeficient (SCID)/ IL-2Rγ knockout (NSG) mice aged 6–8 weeks (purchased from Charles River Laboratories, Wilmington, MA). Mice were initially evaluated after 14 days for engraftment by *in vivo* bioluminescent imaging after the intraperitoneal injection of D-luciferin-K^+ salt bioluminescent substrate (Perkin-Elmer; 150mg/kg) dissolved in 1X PBS with the IVIS Lumina XR (Perkin-Elmer, Shelton, CT, USA). Following initial imaging, mice were randomized into groups of 5 mice injected intraperitonially with vehicle (5% glucose) or dexamethasone (7.5 mg/kg/day) and/or orally gavaged with vehicle (NMP:PEG300 [1:9, v/v]) or BEZ235 (10 mg/kg/day) daily for 7 days. One day after last treatment, mice were reimaged and post-treatment luminescence was compared with initial imaging to determine leukemia progression for each mouse in each treatment group. Radiance was quantified using Living Image Software version 4.3.1 (Perkin-Elmer).

Event-free survival (EFS) in response to treatment was determined in two ALL xenograft models, COG-LL-317x (T-ALL patient-direct xenograft) and RS4;11 (Pre B-ALL). Female non-obese diabetic/severe-combined immunodeficient (NOD/SCID) mice aged 6–8 weeks were purchased from Charles River Laboratories (Wilmington, MA, USA). On the day of inoculation, mice were irradiated (125 cGy of total-body irradiation), and injected via tail vein with either 2×10^6 COG-LL-317x or 8×10^6 RS4;11 cells in 100 μL 1X PBS. After two weeks, engraftment was validated by assessing the percentage of human CD45 in mouse peripheral blood by flow cytometry (>1% confirms engraftment). Treatment consisted of groups of 6–8 mice injected intraperitonially with vehicle (5% glucose) or dexamethasone (15 mg/kg/day as a single agent or 7.5mg/kg/day in combination) and/or orally gavaged with vehicle (NMP:PEG300 [1:9, v/v]) or BEZ235 (10 mg/kg/day) daily for 4 weeks. EFS was

measured from the start date of treatment to the first observation of disease progression or drug-related toxicity (>20% weight loss, lethargy, ruffled fur).

Statistical Analysis

For *in vitro* cytotoxicity experiments, combination indices (CI) were calculated for each fixed-ratio concentration that was used for the cytotoxicity assays using Calcusyn (Biosoft, Cambridge, UK), which numerically quantifies drug synergism based on the multiple drug-effect equation of Chou–Talalay derived from enzyme kinetic methods (30). The synergistic effect of *MCL1* knockdown in combination with dexamethasone was calculated by methods described by Berenbaum (31): Synergy Factor (F_{syn}) = ([Drug $X_{\text{in combination with Y}}$]/[Drug X]) + ([Drug $Y_{\text{in combination with X}}$]/[Drug Y]) (31). *MCL1* siRNA was considered Drug X and dexamethasone was Drug Y. F_{syn} less than 1 indicates synergy. Statistical evaluation of apoptosis, cell cycle progression, gene expression, and *in vivo* leukemia progression was performed using Student's t-test. Tests were considered significant at $P < 0.05$. Mouse EFS was graphically represented by Kaplan–Meier analysis, and survival curves were compared by log-rank test; $P < 0.05$ were considered significant. The plotting and statistical analysis of the data was performed using GraphPad Prism™ (GraphPad Software, La Jolla, CA, USA).

Results

BEZ235 enhances dexamethasone *in vitro* and *in vivo* cytotoxicity preferentially in T-ALL

We first examined the cytotoxic activity of BEZ235 and dexamethasone, as single agents and in combination, in 7 T-ALL cell lines and 5 B-ALL cell lines, all of which express functional GC receptor (Supplementary Fig. 1). BEZ235 noticeably enhanced dexamethasone cytotoxic activity in 5/7 T-ALL models (Fig. 1A). Combination indices (CIs) were calculated for each cell line to determine synergy. In the T-ALL cell lines, those 5/7 models were characterized by a CI value less than 0.3, indicating strong synergy. Four out of five of those synergistic models had CI values less than 0.1, indicating very strong synergy. The two cell lines with non-synergistic CI values, COG-LL-329h and COG-LL-332h, were derived from the same patient at diagnosis and relapse respectively and cytotoxicity appeared to be primarily driven by BEZ235. In primary T-ALL lymphoblasts, BEZ235 plus dexamethasone also demonstrated significantly greater anti-leukemic activity when compared with DMSO, BEZ235, or dexamethasone alone (Fig. 1B, $P<0.01$). Of the B-ALL cell lines, only NALM-6 was characterized by a CI less than 0.3, consistent with our previous data using rapamycin (Fig. 1C) (20). Synergy between BEZ235 and dexamethasone was not observed in the other four B-ALL cell lines. In primary B-ALL lymphoblasts, cytotoxicity appeared to be primarily driven by BEZ235 without a significant increase when combined with dexamethasone (Fig. 1D). Thus, BEZ235 enhances *in vitro* cytotoxic activity of dexamethasone preferentially in T-ALL.

The anti-leukemic activity of BEZ235, dexamethasone, and BEZ235 plus dexamethasone was further assessed in systemic *in vivo* models of T- and B-ALL (T-ALL: COG-LL-317x (patient-derived xenograft) and COG-LL-317h cell line; B-ALL: RS4;11 cell line). *In vivo* activity was first assessed in a systemic bioluminescent model of T-ALL (COG-LL-317h expressing luciferase reporter) where mice were imaged 14 days after inoculation and again

following 7 days of treatment. Initial bioluminescence demonstrated no significant difference in day 0 leukemia burden observed in mice from different treatment groups (Fig. 2A & 2B). Compared with vehicle treated mice, mice with BEZ235 only treatment did not demonstrate significant changes in final leukemia burden. Although mice treated with dexamethasone demonstrated a significant reduction in final leukemia burden compared with control, mice treated with BEZ235 plus dexamethasone showed significantly greater anti-leukemic activity, indicating that BEZ235 enhances dexamethasone anti-leukemic activity *in vivo* models as well. Confirming the *in vivo* bioluminescence results, spleens isolated from mice treated with BEZ235 plus dexamethsone showed significant reduction in weight compared with mice treated with vehicle, BEZ235, or dexamethasone alone (Fig. 2C).

In a separate study, event-free survival (EFS) in response to these agents was assessed in systemic xenograft models of T- and B-ALL. In the systemic T-ALL patient-derived xenograft COG-LL-317x, BEZ235 plus dexamethasone also increased EFS compared with dexamethasone alone (Fig. 2D). While treatment with dexamethasone alone significantly prolonged EFS in the systemic B-ALL model RS4;11, there was no significant increase in survival in mice treated with BEZ235 plus dexamethasone (Fig. 2E).

BEZ235 enhances dexamethasone-induced apoptosis

GCs by themselves exert their anti-leukemic activity through inducing both apoptosis and cell cycle arrest (32). A cell cycle analysis in the COG-LL-317h T-ALL cell line revealed an increase in G_0/G_1 and decrease in S phase cell populations following treatment with BEZ235, dexamethasone, or the BEZ235 plus dexamethasone combination (Supplementary Fig. 2). However, G_0/G_1 arrest was not significantly greater after treatment with BEZ235 plus dexamethasone compared with either single agent alone; indicating the increased cytotoxic activity of BEZ235 plus dexamethasone is not due to cell cycle arrest. Therefore, apoptosis was assessed by measuring Annexin V positivity following treatment with BEZ235, dexamethasone, or BEZ235 plus dexamethasone in T-ALL model COG-LL-317h. As single agents compared with vehicle, only dexamethasone induced a small increase in percentage of apoptotic lymphoblasts (Fig. 3A & 3B). BEZ235 as a single agent had no significant effect on induction of apoptosis compared with vehicle. Treatment with BEZ235 plus dexamethasone, however, significantly increased the percentage of apoptotic lymphoblasts when compared with vehicle, dexamethasone, or BEZ235 alone. In contrast, RS4;11, a dexamethasone-sensitive B-ALL model, demonstrated a robust apoptotic response to dexamethasone alone, but did not further increase with the addition of BEZ235 (Fig. 3A & 3B). Surprisingly, the addition of BEZ235 significantly decreased the percentage of apoptotic lymphoblasts compared with dexamethasone only treated lymphoblasts. In COG-LL-317h, activation of caspases 9 and 3 were assessed following treatment by western blotting for their respective cleavage products. Treatment with BEZ235 plus dexamethasone led to increased cleavage of both caspase 9 and caspase 3 while no cleavage of caspases was detected in BEZ235, dexamethasone, or vehicle treated lymphoblasts (Fig. 3C). These data show that BEZ235 plus dexamethasone anti-leukemic activity is primarily working through increasing apoptosis.

BEZ235 enhances dexamethasone-induced apoptosis through increased expression of the pro-apoptotic BCL-2 protein BIM

The pro-apoptotic BCL-2 family protein BIM (encoded by *BCL2L11*) is an indirect glucocorticoid target and major mediator of glucocorticoid-induced apoptosis (33–37). Consequently, in both preclinical models and primary lymphoblasts, there are inferior responses to GCs and poorer prognosis associated with reduced increases in BIM expression following GC exposure (38, 39). We therefore examined the effect of BEZ235 on dexamethasone-induced BIM expression in the BEZ235 plus dexamethasone responsive T-ALL cell line COG-LL-317h following treatment and compared with the dexamethasone-sensitive B-ALL cell line RS4;11. After treating COG-LL-317h lymphoblasts with BEZ235, dexamethasone, or BEZ235 plus dexamethasone, there was an observed increase in expression of the three dominant isoforms of BIM with BEZ235 plus dexamethasone treatment compared with dexamethasone only treament at both 24 and 36 hours (Fig. 4A). Correspondingly, this was associated with a BEZ235 plus dexamethasone combination-induced increase in *BCL2L11* also at 24 and 36 hours (Fig. 4B). The increase in BIM expression was also observed in two other BEZ235 plus dexamethasone combination responsive T-ALL cell lines (CCRF-CEM and TX-LY-172h) demonstrating it to be a common response in T-ALL models (Fig. 4A). In contrast to this observation, the B-ALL cell line RS4;11, showed increases in the three BIM isoforms when treated with dexamethasone, but BIM expression was not further increased with BEZ235 plus dexamethasone (Fig. 4C). In fact, there was a decrease in BIM expression at all three time points, which is consistent with the reduction in apoptosis seen earlier. *BCL2L11* expression, however, was not significantly different between dexamethasone and BEZ235 plus dexamethasone treated lymphoblasts, indicating that the further decrease in BIM protein following treatment with BEZ235 plus dexamethasone relative to dexamethasone alone is due to the changes in stability of the protein (Fig. 4D). A similar trend was observed in another BALL cell line COG-LL-319h, although dexamethasone had minimal impact on BIM expression as a single agent (Fig. 4C). Splenic tissue isolated from mice engrafted with COG-LL-317h and treated with agents for 7 days were fixed and stained with antibody against BIM. Mice treated with BEZ235 plus dexamethasone demonstrated increased BIM staining compared to mice treated with vehicle or either single agent alone, consistent with data obtained from *in vitro* studies (Fig. 4E).

As BIM (encoded by *BCL2L11*) is necessary for dexamethasone-induced apoptosis, we investigated whether it contributes to BEZ235 plus dexamethasone anti-leukemic activity. Using a small-interfering RNA (siRNA) against *BCL2L11*, *BCL2L11* was knocked-down in COG-LL-317h (Fig. 5A) and the changes in apoptosis and cytotoxicity in response to BEZ235, dexamethasone, or BEZ235 plus dexamethasone were observed. Following treatment with BEZ235 plus dexamethasone, *BCL2L11* knockdown lymphoblasts showed a significant reduction in caspase 3 cleavage compared with non-targeting siRNA control (Fig. 5A). Correspondingly, both apoptosis (Fig. 5B) and cytotoxicity (Fig. 5C) were significantly reduced following treatment with BEZ235 plus dexamethasone in *BCL2L11* knockdown lymphoblasts when compared with non-targeting siRNA control.

AKT1 inhibition alleviates suppression of basal and dexamethasone-induced BIM expression

PTEN inactivation/deletion and concomitant PI3K/AKT/mTOR pathway activation are common abnormalities in primary T-ALL (9). Therefore, we investigated the role of PTEN status and PI3K/AKT pathway activity on GC responses in T- and B-ALL cell lines. We examined PTEN protein expression in 5 patient-derived T-ALL cell lines (COG-LL-329h and COG-LL-332h as well as MOLT3 and MOLT-4 were derived from the same patients) and compared with 5 patient-derived B-ALL cell lines (Supplementary Fig. 3A). Analysis of PTEN protein expression in ALL cell lines revealed undetectable protein in 3 out of 5 T-ALL (COG-LL-317h, CCRF-CEM, MOLT-4) models examined. Sequence analysis of exon 5 and exon 7 revealed truncating mutations in each of those three cell lines (Supplementary Table 1). COG-LL-332h had a substantial reduction in PTEN expression and TX-LY-172h demonstrated comparable levels in expression when compared with B-ALL cell lines. The T-ALL models with undetectable levels of PTEN by western blotting demonstrated substantially increased phosphorylation of AKT at both Thr308 and Ser473. COG-LL-332h, which shows reduced PTEN expression, has a comparable level of AKT phosphorylation compared with B-ALL cell lines, suggesting that even small amount of PTEN is enough to limit phosphorylation of AKT. TX-LY-172h, however, which has functional PTEN, has comparable AKT phosphorylation compared with B-ALL cell lines which suggests that BEZ235 plus dexamethasone synergistic activity is not dependent on mutated PTEN or hyperphosphorylated AKT. There were no mutations identified in *AKT1, PIK3CA* (p110α exon 9 and 20), or *RPS6KB1* (S6 Kinase) in the cell lines used for these experiments (Supplementary Table 1).

Interestingly we found an inverse association between AKT phosphorylation and BIM protein expression. COG-LL-317h, MOLT-4, and CCRF-CEM, three PTEN-null T-ALL cell lines, all showed lower BIM compared with B-ALL cell lines. Relatively lower basal BIM expression was noted in glucocorticoid-insensitive T-ALL MOLT-3, Jurkat, and SUP-T1 T-ALL models (data not shown) which also demonstrated substantial AKT hyperphosphorylation, suggesting GC resistance is mediated downstream of AKT. As a downstream target of AKT and target of BEZ235, we also investigated the phosphorylation status of mTOR complex 1 (mTORC1) substrates S6K1 and 4EBP1 in T- and B-ALL models as mTORC1 activity could account for BIM suppression as well. However, a noticeable association between mTORC1 activation of BIM expression was not observed, suggesting that AKT primarily mediates suppression of GC-induced apoptosis (Supplementary Fig. 3).

Although BEZ235 inhibits phosphorylation and activation of various components of the PI3K/AKT/mTOR pathway, there are limited data describing the effects GCs have on this pathway in human ALL. To demonstrate the effect of dexamethasone, BEZ235, and BEZ235 plus dexamethasone on this pathway, COG-LL-317h lymphoblasts were treated for 12, 24, and 36 hours before assessing expression and phosphorylation status of AKT, FOXO, mTOR, S6K1, S6, and 4EBP1 (Supplementary Fig. 3B). Interestingly, with dexamethasone treatment, we found a time-dependent increase in phosphorylation of AKT at both Ser473 and Thr308. BEZ235 as a single agent and in combination with

dexamethasone potently reduced phosphorylation of AKT at both sites to undetectable levels as well as one of its targets FOXO4. In contrast, mTORC1 activity as indicated by phosphorylation of its target, S6K1 showed a time-dependent reduction in phosphorylation by dexamethasone alone. The ability of dexamethasone to reduce activation of mTORC1 and its targets further provide evidence that AKT plays a role in glucocorticoid resistance.

Of the three AKT isoforms, AKT1 is the most dominant isoform expressed ubiquitously throughout all tissues and thought to be the primary isoform involved in regulating cell survival (40). To investigate the role of AKT1 on dexamethasone activity, COG-LL-317h lymphoblasts were transfected with siRNA specifically against *AKT1*. *AKT1* knockdown decreased AKT activity for at least 48 hours (Fig. 5D). Compared with non-targeting control siRNA, siRNA against *AKT1* demonstrated increased expression of the 3 BIM isoforms following 24 hours of dexamethasone or BEZ235 plus dexamethasone treatment (Fig. 5E). Despite observing an increase in BIM, however, *AKT1* knockdown led to only a minimal, but statistically significant increase in dexamethasone or BEZ235 plus dexamethasone cytotoxicity (Supplementary Fig. 4A). Nonetheless, this demonstrated AKT1 plays a role in suppressing dexamethasone-induced BIM expression in COG-LL-317h.

MCL-1 downregulation by BEZ235 increases dexamethasone response in T-ALL

With only a modest increase in dexamethasone cytotoxicity after *AKT1* knockdown, it is likely that another mechanism plays a role in BEZ235 plus dexamethasone cytotoxicity. It has been previously suggested that the anti-apoptotic BCL-2 family protein MCL-1 plays a role in glucocorticoid resistance in ALL (41, 42). In our studies, when comparing BIM protein expression between COG-LL-317h and RS4;11 after treatment with BEZ235, dexamethasone, or BEZ235 plus dexamethasone, the increased BIM expression observed after treatment in COG-LL-317h was less than basal expression of BIM in RS4;11, suggesitng that increasing BIM, although necessary, is not sufficient to induce apoptosis in models with hyperphosphorylated AKT (Supplementary Fig. 4B). We therefore hypothesized that the increased glucocorticoid-induced BIM expression following *AKT1* knockdown is being sequestered by MCL-1, further inhibiting the ability to induce dexamethasone-induced apoptosis. No distinctive differences were seen in constitutive MCL-1 levels between sensitive and insensitive cell lines or T- and B-ALL cell lines (Fig. 6A). However, as observed with various other PI3K/AKT/mTOR pathway inhibitors (43, 44), a strong reduction in MCL-1 expression was observed in COG-LL-317h following treatment with BEZ235, suggesting MCL-1 plays a role in the BEZ235 plus dexamethasone cytotoxic activity in our models (Fig. 6B). RT-PCR of *MCL1* demonstrated modest increases in *MCL1* expression, indicating that BEZ235 regulates MCL-1 post-transcriptionally (Supplementary Fig. 4C). Other BCL-2 family proteins, such as BCL-2 and BCL-xL have also been implicated in preventing glucocorticoid-induced apoptosis (42); however, in COG-LL-317h, BEZ235 did not cuase any substantial changes in BCL-2 expression and BCL-xL was under the measurable level by western blotting, suggesting they do not have a significant role in the combination mechanism in this model (Fig. 6B). Knockdown of *MCL1* by siRNA increased dexamethasone-induced cytotoxicity (Supplementary Fig. 4D). Additionally, *MCL1* knockdown was able to induce apoptosis and enhance dexamethasone-induced apoptosis (Fig. 6D). Despite the ability of BEZ235 to

decrease MCL-1 protein expression, *AKT1* knockdown was unable to recapitulate this effect (Supplementary Fig. 4E), suggesting AKT1 inhibition is not regulating MCL-1 and explains the lack of robust cytotoxic response observed previously. As MCL-1 can bind to and sequester BIM, we treated COG-LL-317h with BEZ235, dexamethasone, or BEZ235 plus dexamethasone before immunoprecipitating for MCL-1. Immunoprecipitation of MCL-1 confirmed that MCL-1 was interacting with BIM in our model and the increased BIM due to dexamethasone or BEZ235 plus dexamethasone treatment was also being sequestered by MCL-1 (Fig. 4E), indicating that MCL-1 is also playing a role in GC resistance. BEZ235 treatment also decreased MCL-1 protein expression in RS4;11 lymphoblasts (Supplementary Fig. 5A), but *MCL1* knockdown by siRNA in RS4;11 (Supplementary Fig. 5B) did not significantly increase apoptosis (Supplementary Fig. 5C). Similarly, *MCL1* knockdown led to small increases in dexamethasone cytotoxicity, but demonstrated only small effects at clinically achievable concentrations of dexamethasone (Supplementary Fig. 5D). These data suggest that decreased MCL-1, although a common effect of BEZ235 across different ALL cell lines, only alters apoptotic response and cytotoxicity in models with low BIM expression and *PTEN* mutations.

Discussion

Glucocorticoid resistance in the treatment of pediatric ALL remains a major clinical problem and several mechanisms have been suggested (45). Despite the widespread use of GCs in the treatment of ALL as well as other conditions, our understanding of the molecular basis of their function remains unclear. Our results indicate AKT1 is partially responsible for suppression of GC-induced apoptotic pathways leading to decreases in BIM expression, a known mediator of GC-induced apoptosis, which is consistent with previous studies implicating AKT in GC resistance and suppression of BIM expression in T-ALL models (46, 47). We also examined the downstream activation of mTORC1 and observed that dexamethasone was able to reduce mTORC1 activation independent of AKT. The observation of increased AKT phosphorylation upon dexamethasone treatment may indicate there is activation of the known negative feedback loop consisting of S6K1 phosphorylation and downregulation of IRS1 (48). This activity could also contribute to GC resistance by increasing AKT activation and therefore further inhibiting apoptosis, and warrants further investigation. It is also worth noting that inhibition of mTORC1 by dexamethasone treatment over time correlated with progressive G_0/G_1 arrest, suggesting that mTORC1 inhibition may be involved in the cytostatic effects of GCs. This would indicate that the cytotoxic and cytostatic mechanisms of GCs may be independent of each other.

The PI3K/AKT pathway appears to play a critical role in T-ALL as common mutations in T-ALL (*NOTCH1*/*PTEN*) can lead to constitutive activation of this pathway and could account for the high frequency of AKT activation observed in primary T-ALL patient samples (15). This is particularly highlighted by the contrast in cytotoxic activity observed between T-ALL and B-ALL models in response to treatment with BEZ235 plus dexamethasone. In T-ALL models, BEZ plus dexamethasone synergistic activity appeared to be independent of PTEN or AKT status, as evidenced by the increased BIM expression and cytotoxic activity observed in TX-LY-172h, a PTEN wild-type T-ALL model, suggesting BEZ235 plus dexamethasone synergistc activity is not dependent on presence of PI3K/AKT pathway

activation. The two T-ALL cell lines without synergistic activity, COG-LL-329h and COG-LL-332h, are derived from the same patient at different phases in treatment and have minimal GC receptor expression, suggesting that there may be AKT-independent mechanism's of GC resistance. In contrast, increased cytotoxic activity with BEZ235 plus dexamethasone was not observed in B-ALL models. An exception, NALM-6, a B-ALL model with synergistic activity, did not demonstrate increased BEZ235 plus dexamethasone-induced BIM expression, suggesting unique molecular characteristics of this model are responsible for the increased cytotoxicity observed with BEZ235 plus dexamethasone. Additionally, BEZ235 plus dexamethasone may be antagonistic in some BALL models, as demonstrated in RS4;11 and COG-LL-319h, further demonstrating the applicability of this drug combination is in T-ALL only.

Although BEZ235 increased dexamethasone cytotoxic activity in T-ALL models independent of PTEN function, PTEN-null cell lines had substantial reductions in basal BIM expression (Supplemenaty Fig. 3). In addition, reductions in BIM expression was associated with considerable AKT phosphorylation. This agrees with a recent study implicating Akt2 overexpression with reduction in BIM expression in a zebrafish T-ALL model (47). Despite inhibition of AKT with BEZ235, in PTEN-null cell lines, we were unable to reconstitute BIM expression to levels similar to wild-type PTEN ALL cells (Supplementary Fig. 3), which may indicate long-term constitutive activation of AKT results in suppression of BIM expression that is not completely reversed by inhibition of AKT. In addition, AKT1 knockdown in PTEN-null T-ALL model COG-LL-317h increased both dexamethasone- and BEZ235 plus dexamethasone-induced expression of BIM, but only minimally increased the cytotoxic effect. This may provide a challenge when developing PI3K/AKT pathway inhibitors for the clinical treatment of pediatric ALL; as GC resistance cannot be completely reversed by inhibiting AKT. Alternatively, inhibition of the PI3K/AKT/mTOR pathway has also been shown to decrease MCL-1 protein expression in murine-derived B-cell (43), multiple myeloma (44), and ALL cell lines (19). Our data demonstrated a BEZ235 decreased MCL-1 expression in ALL cell line models. This ability of BEZ235 to reduce MCL-1 expression could account for the inability of *AKT1* knockdown to substantially increase dexamethasone- and BEZ235 plus dexamethasone-induced cytotoxicity as *AKT1* knockdown alone failed to substantially decrease MCL-1. MCL-1 can bind to and sequester BIM (19, 42), and thus by decreasing MCL-1 by BEZ235 treatment there is increased availability of free BIM to induce apoptosis as demonstrated with BEZ235 plus dexamethasone treatment. In T-ALL with substantial reductions in BIM, as observed in PTEN-null models, this may be necessary to achieve GC-induced apoptosis and explains why *AKT1* knockdown was insufficient to induce apoptosis in PTEN-null T-ALL. As suggested by Ploner et al., by regulation of a "BCL-2 rheostat" we may be able to enhance GC responses in GC resistant ALL (42).

BEZ235 potentiates dexamethasone cytotoxicity in models of T-ALL by increasing BIM and decreasing MCL-1, providing a possible adjunct in current T-ALL treatment protocols (Mechanism summarized in Supplementary Fig. 6). Our data are in agreement with a previous cell line-study of BEZ235 as a potential therapy modifier in GC resistant T-ALL (49). Mechanistically, AKT1 plays a role in suppressing GC-induced apoptotic pathways,

yet the precise AKT1 target remains unclear. Piovan et al. have implicated direct phosphorylation of the GC receptor as a mechanism of PI3K/AKT pathway mediated GC resistance and may be a plausible mechanism of action for BEZ235 plus dexamethasone (46). Nonetheless, discovery of this mechanism may provide information about possible therapeutic targets to overcome GC resistance while minimizing adverse effects. These data in concert with other studies demonstrating increased activity observed with PI3K/AKT pathway inhibitors in combination with glucocorticoids (19, 20, 46) provide a novel approach to overcoming glucocorticoid resistance in T-ALL. If additional studies in T-ALL xenograft of a PI3K/AKT pathway inhibitor + glucocorticoids confirm the data presentd here, early-phase clinical trials of such a combination should be undertaken.

Supplementary Material

Refer to Web version on PubMed Central for supplementary material.

Acknowledgments

The authors would like to thank Novartis Pharmaceuticals for supplying BEZ235. The authors thank the Children's Oncology Group (COG) and the Texas Cancer Cell Repository (TXCCR) for providing cell line and xenograft models, and Dr. Donald Kohn for supplying the pCCL-c-MNDU3c-LUC-PGK-hB7 vector. This work was funded by an R15 grant from the National Institute of Health (NIH) to MK (1R15CA159308-01). CH received support from the Achievement Rewards for College Scientists (ARCS) Foundation and AT&T Foundation.

References

1. Hyman CB, Sturgeon P. Prednisone therapy of acute lymphatic leukemia in children. Cancer. 1956; 9:965–70. [PubMed: 13364883]
2. Pui CH, Evans WE. Treatment of acute lymphoblastic leukemia. New England Journal of Medicine. 2006; 354:166–78. [PubMed: 16407512]
3. Dordelmann M, Reiter A, Borkhardt A, Ludwig WD, Gotz N, Viehmann S, et al. Prednisone response is the strongest predictor of treatment outcome in infant acute lymphoblastic leukemia. Blood. 1999; 94:1209–17. [PubMed: 10438708]
4. Riehm H, Reiter A, Schrappe M, Berthold F, Dopfer R, Gerein V, et al. Corticosteroid-dependent reduction of leukocyte count in blood as a prognostic factor in acute lymphoblastic leukemia in childhood (therapy study ALL-BFM 83). Klin Padiatr. 1987; 199:151–60. [PubMed: 3306129]
5. Schrappe M, Reiter A, Zimmermann M, Harbott J, Ludwig WD, Henze G, et al. Long-term results of four consecutive trials in childhood ALL performed by the ALL-BFM study group from 1981 to 1995. Berlin-Frankfurt-Munster Leukemia. 2000; 14:2205–22. [PubMed: 11187912]
6. Engelman JA. Targeting PI3K signalling in cancer: opportunities, challenges and limitations. Nat Rev Cancer. 2009; 9:550–62. [PubMed: 19629070]
7. McCubrey JA, Steelman LS, Kempf CR, Chappell WH, Abrams SL, Stivala F, et al. Therapeutic resistance resulting from mutations in Raf/MEK/ERK and PI3K/PTEN/Akt/mTOR signaling pathways. J Cell Physiol. 2011; 226:2762–81. [PubMed: 21302297]
8. Barrett D, Brown VI, Grupp SA, Teachey DT. Targeting the PI3K/AKT/mTOR signaling axis in children with hematologic malignancies. Paediatr Drugs. 2012; 14:299–316. [PubMed: 22845486]
9. Gutierrez A, Sanda T, Grebliunaite R, Carracedo A, Salmena L, Ahn Y, et al. High frequency of PTEN, PI3K, and AKT abnormalities in T-cell acute lymphoblastic leukemia. Blood. 2009; 114:647–50. [PubMed: 19458356]
10. Jotta PY, Ganazza MA, Silva A, Viana MB, da Silva MJ, Zambaldi LJ, et al. Negative prognostic impact of PTEN mutation in pediatric T-cell acute lymphoblastic leukemia. Leukemia. 2010; 24:239–42. [PubMed: 19829307]

11. Larson GA, Chen Q, Kugel DS, Ge Y, LaFiura K, Haska CL, et al. The impact of NOTCH1, FBW7 and PTEN mutations on prognosis and downstream signaling in pediatric T-cell acute lymphoblastic leukemia: a report from the Children's Oncology Group. Leukemia. 2009; 23:1417–25. [PubMed: 19340001]
12. Silva A, Yunes JA, Cardoso BA, Martins LR, Jotta PY, Abecasis M, et al. PTEN posttranslational inactivation and hyperactivation of the PI3K/Akt pathway sustain primary T cell leukemia viability. J Clin Invest. 2008; 118:3762–74. [PubMed: 18830414]
13. Morishita N, Tsukahara H, Chayama K, Ishida T, Washio K, Miyamura T, et al. Activation of Akt is associated with poor prognosis and chemotherapeutic resistance in pediatric B-precursor acute lymphoblastic leukemia. Pediatr Blood Cancer. 2012; 59:83–9. [PubMed: 22183914]
14. Weng AP, Ferrando AA, Lee W, Morris JP, Silverman LB, Sanchez-Irizarry C, et al. Activating mutations of NOTCH1 in human T cell acute lymphoblastic leukemia. Science. 2004; 306:269–71. [PubMed: 15472075]
15. Palomero T, Sulis ML, Cortina M, Real PJ, Barnes K, Ciofani M, et al. Mutational loss of PTEN induces resistance to NOTCH1 inhibition in T-cell leukemia. Nat Med. 2007; 13:1203–10. [PubMed: 17873882]
16. Bandapalli OR, Zimmermann M, Kox C, Stanulla M, Schrappe M, Ludwig WD, et al. NOTCH1 activation clinically antagonizes the unfavorable effect of PTEN inactivation in BFM-treated children with precursor T-cell acute lymphoblastic leukemia. Haematologica. 2013; 98:928–36. [PubMed: 23349303]
17. Song MS, Salmena L, Pandolfi PP. The functions and regulation of the PTEN tumour suppressor. Nat Rev Mol Cell Biol. 2012; 13:283–96. [PubMed: 22473468]
18. Manning BD, Cantley LC. AKT/PKB signaling: navigating downstream. Cell. 2007; 129:1261–74. [PubMed: 17604717]
19. Wei G, Twomey D, Lamb J, Schlis K, Agarwal J, Stam RW, et al. Gene expression-based chemical genomics identifies rapamycin as a modulator of MCL1 and glucocorticoid resistance. Cancer Cell. 2006; 10:331–42. [PubMed: 17010674]
20. Zhang C, Ryu YK, Chen TZ, Hall CP, Webster DR, Kang MH. Synergistic activity of rapamycin and dexamethasone in vitro and in vivo in acute lymphoblastic leukemia via cell-cycle arrest and apoptosis. Leuk Res. 2012; 36:342–9. [PubMed: 22137317]
21. Wunderle L, Badura S, Lang F, et al. Safety and Efficacy Of BEZ235, a Dual PI3-Kinase/mTOR Inhibitor, In Adult Patients With Relapsed Or Refractory Acute Leukemia: Results Of a Phase I Study. Blood. 2013; 122:2675.
22. Maira SM, Stauffer F, Brueggen J, Furet P, Schnell C, Fritsch C, et al. Identification and characterization of NVP-BEZ235, a new orally available dual phosphatidylinositol 3-kinase/ mammalian target of rapamycin inhibitor with potent in vivo antitumor activity. Mol Cancer Ther. 2008; 7:1851–63. [PubMed: 18606717]
23. Salkeni MA, Rixe O, Abdel Karim N, et al. BEZ235 in combination with everolimus for advanced solid malignancies: Preliminary results of a phase Ib dose-escalation study. J of Clin Oncology. 2013; 31(suppl; abstr e13518)
24. Krop IE, Saura C, Rodon Ahnert J, Becerra C, Britten CD, Isakoff SJ, et al. A phase I/IB dose-escalation study of BEZ235 in combination with trastuzumab in patients with PI3-kinase or PTEN altered HER2+ metastatic breast cancer. J Clin Oncol (Meeting Abstracts). 2012; 30:508.
25. Arkenau HT, Jones SF, Kurkjian C, Infante JR, Pant S, Burris HA, et al. The PI3K/mTOR inhibitor BEZ235 given twice daily for the treatment of patients (pts) with advanced solid tumors. J Clin Oncol (Meeting Abstracts). 2012; 30:3097.
26. Brown JM, Lemmon MJ. Tumor hypoxia can be exploited to preferentially sensitize tumors to fractionated irradiation. International Journal of Radiation Oncology, Biology, Physics. 1991; 20:457–61.
27. Sheard MA, Ghent MV, Cabral DJ, Lee JC, Khankaldyyan V, Ji L, et al. Preservation of high glycolytic phenotype by establishing new acute lymphoblastic leukemia cell lines at physiologic oxygen concentration. Experimental Cell Research. (in press).

28. Frgala T, Kalous O, Proffitt RT, Reynolds CP. A fluorescence microplate cytotoxicity assay with a 4-log dynamic range that identifies synergistic drug combinations. Mol Cancer Ther. 2007; 6:886–97. [PubMed: 17363483]
29. Georgakis GV, Li Y, Rassidakis GZ, Medeiros LJ, Mills GB, Younes A. Inhibition of the phosphatidylinositol-3 kinase/Akt promotes G1 cell cycle arrest and apoptosis in Hodgkin lymphoma. Br J Haematol. 2006; 132:503–11. [PubMed: 16412023]
30. Chou TC, Talalay P. Quantitative analysis of dose-effect relationships: the combined effects of multiple drugs or enzyme inhibitors. Adv Enzyme Regul. 1984; 22:27–55. [PubMed: 6382953]
31. Berenbaum MC. Synergy, additivism and antagonism in immunosuppression. A critical review Clin Exp Immunol. 1977; 28:1–18.
32. Greenstein S, Ghias K, Krett NL, Rosen ST. Mechanisms of glucocorticoid-mediated apoptosis in hematological malignancies. Clin Cancer Res. 2002; 8:1681–94. [PubMed: 12060604]
33. Bachmann PS, Gorman R, Mackenzie KL, Lutze-Mann L, Lock RB. Dexamethasone resistance in B-cell precursor childhood acute lymphoblastic leukemia occurs downstream of ligand-induced nuclear translocation of the glucocorticoid receptor. Blood. 2005; 105:2519–26. [PubMed: 15572593]
34. Wang Z, Malone MH, He H, McColl KS, Distelhorst CW. Microarray analysis uncovers the induction of the proapoptotic BH3-only protein Bim in multiple models of glucocorticoid-induced apoptosis. J Biol Chem. 2003; 278:23861–7. [PubMed: 12676946]
35. Thompson EB, Johnson BH. Regulation of a distinctive set of genes in glucocorticoid-evoked apoptosis in CEM human lymphoid cells. Recent Prog Horm Res. 2003; 58:175–97. [PubMed: 12795419]
36. Abrams MT, Robertson NM, Yoon K, Wickstrom E. Inhibition of glucocorticoid-induced apoptosis by targeting the major splice variants of BIM mRNA with small interfering RNA and short hairpin RNA. J Biol Chem. 2004; 279:55809–17. [PubMed: 15509554]
37. Zhang L, Insel PA. The pro-apoptotic protein Bim is a convergence point for cAMP/protein kinase A- and glucocorticoid-promoted apoptosis of lymphoid cells. J Biol Chem. 2004; 279:20858–65. [PubMed: 14996839]
38. Bachmann PS, Gorman R, Papa RA, Bardell JE, Ford J, Kees UR, et al. Divergent mechanisms of glucocorticoid resistance in experimental models of pediatric acute lymphoblastic leukemia. Cancer Res. 2007; 67:4482–90. [PubMed: 17483364]
39. Jiang N, Koh GS, Lim JY, Kham SK, Ariffin H, Chew FT, et al. BIM is a prognostic biomarker for early prednisolone response in pediatric acute lymphoblastic leukemia. Exp Hematol. 2011; 39:321–9. 329. [PubMed: 21130142]
40. Chen WS, Xu PZ, Gottlob K, Chen ML, Sokol K, Shiyanova T, et al. Growth retardation and increased apoptosis in mice with homozygous disruption of the Akt1 gene. Genes Dev. 2001; 15:2203–8. [PubMed: 11544177]
41. Stam RW, den Boer ML, Schneider P, de BJ, Hagelstein J, Valsecchi MG, et al. Association of high-level MCL-1 expression with in vitro and in vivo prednisone resistance in MLL-rearranged infant acute lymphoblastic leukemia. Blood. 2010; 115:1018–25. [PubMed: 19965632]
42. Ploner C, Rainer J, Niederegger H, Eduardoff M, Villunger A, Geley S, et al. The BCL2 rheostat in glucocorticoid-induced apoptosis of acute lymphoblastic leukemia. Leukemia. 2008; 22:370–7. [PubMed: 18046449]
43. Maurer U, Charvet C, Wagman AS, Dejardin E, Green DR. Glycogen synthase kinase-3 regulates mitochondrial outer membrane permeabilization and apoptosis by destabilization of MCL-1. Mol Cell. 2006; 21:749–60. [PubMed: 16543145]
44. Sinnberg T, Lasithiotakis K, Niessner H, Schittek B, Flaherty KT, Kulms D, et al. Inhibition of PI3K-AKT-mTOR signaling sensitizes melanoma cells to cisplatin and temozolomide. J Invest Dermatol. 2009; 129:1500–15. [PubMed: 19078992]
45. Bhadri VA, Trahair TN, Lock RB. Glucocorticoid resistance in paediatric acute lymphoblastic leukaemia. J Paediatr Child Health. 2012; 48:634–40. [PubMed: 22050419]
46. Piovan E, Yu J, Tosello V, Herranz D, Ambesi-Impiombato A, Da Silva AC, et al. Direct reversal of glucocorticoid resistance by AKT inhibition in acute lymphoblastic leukemia. Cancer Cell. 2013; 24:766–76. [PubMed: 24291004]

47. Reynolds C, Roderick JE, LaBelle JL, Bird G, Mathieu R, Bodaar K, et al. Repression of BIM mediates survival signaling by MYC and AKT in high-risk T-cell acute lymphoblastic leukemia. Leukemia. 2014; 28:1819–27. [PubMed: 24552990]

48. Ma XM, Blenis J. Molecular mechanisms of mTOR-mediated translational control. Nat Rev Mol Cell Biol. 2009; 10:307–18. [PubMed: 19339977]

49. Schult C, Dahlhaus M, Glass A, Fischer K, Lange S, Freund M, et al. The dual kinase inhibitor NVP-BEZ235 in combination with cytotoxic drugs exerts anti-proliferative activity towards acute lymphoblastic leukemia cells. Anticancer Res. 2012; 32:463–74. [PubMed: 22287733]

Statement of Translational Relevance

Glucocorticoids represent a critical component of pediatric acute lymphoblastic leukemia (ALL) treatment as glucocorticoid resistance has been associated with poor outcomes. T-cell ALL (TALL) frequently manifests constitutive activation of the PI3K/AKT/mTOR pathway which may contribute to the glucocorticoid resistance observed in these patients. We demonstrated that PI3K/mTOR inhibitor BEZ235 potentiates dexamethasone cytotoxic activity in a panel of T-ALL cell line and xenograft models. BEZ235, through inhibition of AKT1, increased expression of pro-apoptotic protein BIM. BEZ235, independently of AKT, also decreased expression of anti-apoptotic protein MCL-1. In addition to demonstrating BEZ235 to be a possible adjunct to glucocorticoid treatment in T-ALL, identification of BIM and MCL-1 as important molecular mediators of drug sensitivity informs future studies seeking to improve glucocorticoid cytotoxic activity in T-cell ALL.

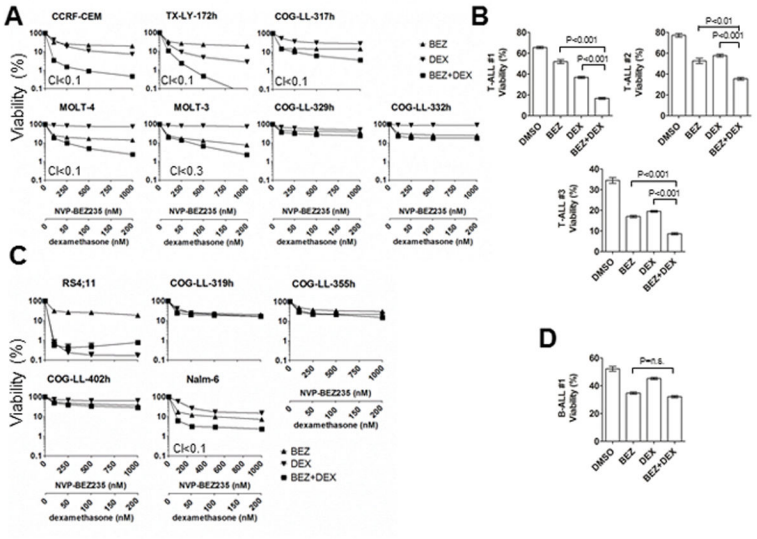

Figure 1. BEZ235 enhances Dexamethasone cytotoxicity in several T-ALL models

(A) and **(C)** Dose response curves for 7 T-ALL cell lines **(A)** and 5 B-ALL cell lines **(C)** exposed to BEZ235 (BEZ; dose range: 100–1000 nM), dexamethasone (DEX, dose range: 20–200 nM), or BEZ235 plus dexamethasone (BEZ+DEX; dose range: 100–1000nM and 20–200 nM, respectively) at a fixed ratio. Cytotoxicity was evaluated after 72 hours of exposure by DIMSCAN and relative survival (%) was determined by mean fluorescence of the treated cells/mean fluorescence of control cells x 100. Combination index (CI) values are displayed for cell lines displaying strong synergy (CI<0.3). Each point represents mean ± SD. **(B)** and **(D)** Primary T- **(B)** and B-ALL cells **(D)** were treated with BEZ235 (1μM), dexamethasone (200nM), or BEZ235 plus dexamethasone (1μM and 200nM, respectively) for 36 hours. Cells were stained for anti-Annexin V-FITC conjugated antibody and propidium iodide before analysis by flow cytometry. Viability (%) represents percentage of cells not staining for Annexin V or propidium iodide. Bar graphs represent mean ± standard deviation.

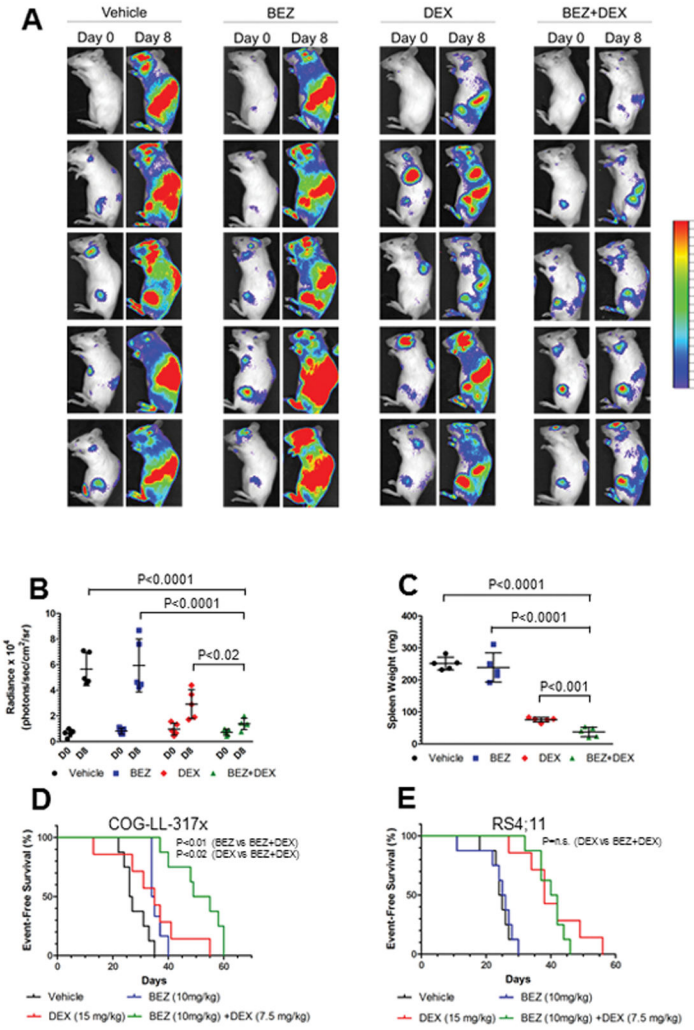

Figure 2. BEZ235 enhances dexamethasone activity in T-ALL xenograft models

(A) Bioluminescent images of NSG mice engrafted with COG-LL-317h cells expressing luciferase before (Day 0) and after (Day 8) treatment with vehicle (NMP:PEG300 [1:9, v/v] via oral gavage + 5% glucose via intraperitoneal injection), BEZ235 (10 mg/kg via oral gavage), dexamethasone (7.5 mg/kg via intraperitoneal injection), or BEZ235 (10 mg/kg) + dexamethasone (7.5 mg/kg). **(B)** Quantitative analysis of tumor load in COG-LL-317h engrafted mice as estimated by *in vivo* bioluminescence at day 0 and day 8 for mice treated with vehicle, BEZ235, dexamethasone, or BEZ235 + dexamethasone. Results are reported in units of radiance (photons/second/cm^2/steradian). Black lines represent mean ± standard deviation for each group. **(C)** Quantification of tumor burden as estimated by spleen weight in COG-LL-317h engrafted mice following 7 days of treatment. Black lines represent mean ± standard deviation for each group. **(D)** Event-free survival for mice engrafted with COG-LL-317x after 28 days of treatment with vehicle (n=8), BEZ235 (10 mg/kg; n=6), dexamethasone (15 mg/kg; n=7), or BEZ235 plus dexamethasone (10 mg/kg and 7.5 mg/kg respectively; n=8). **(E)** Event-free survival for mice engrafted with RS4;11 after 28 days of

treatment with vehicle (n=8), BEZ235 (10 mg/kg; n=8), dexamethasone (15 mg/kg; n=7), or BEZ235 plus dexamethasone (10 mg/kg and 7.5 mg/kg respectively; n=8).

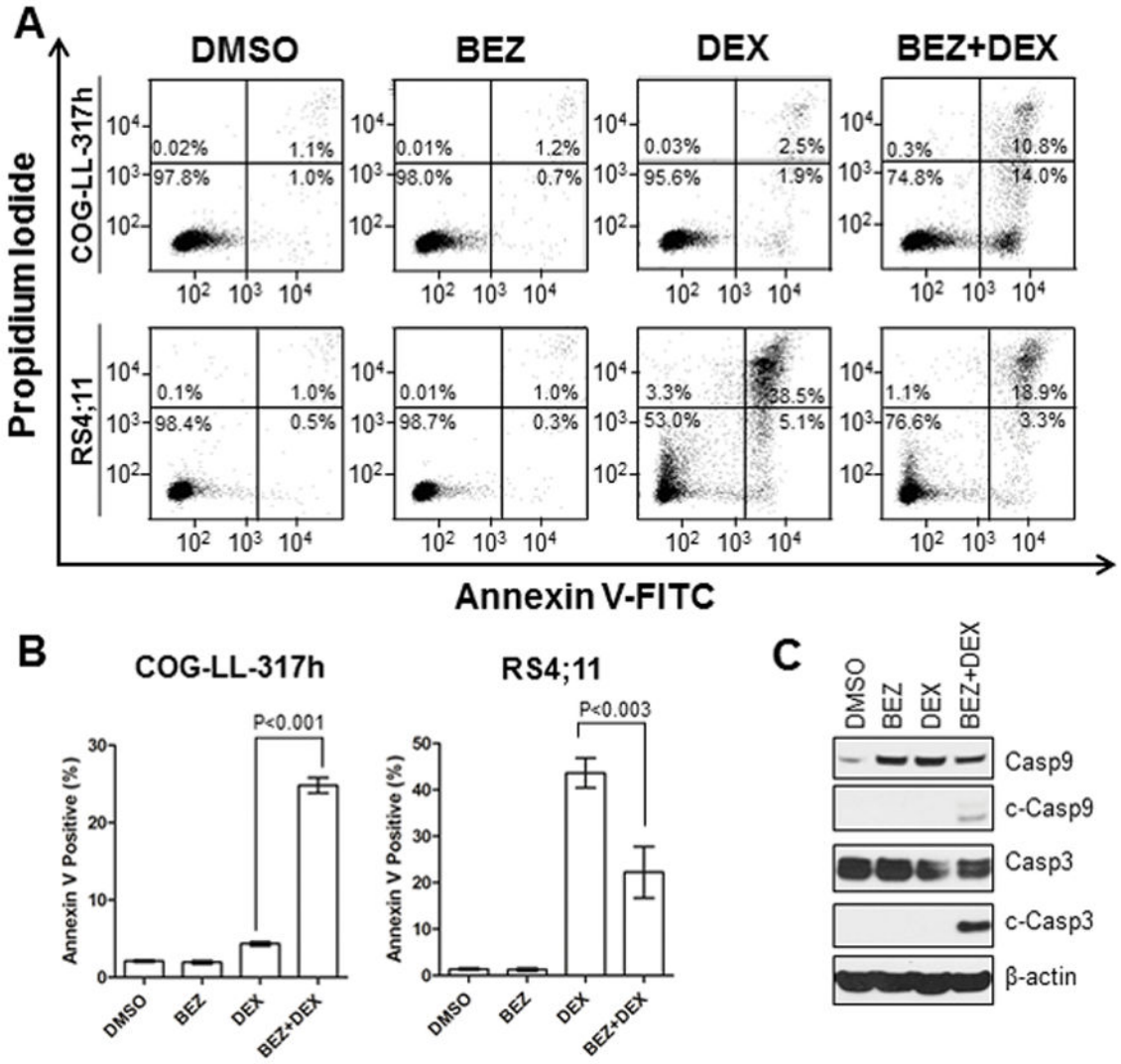

Figure 3. BEZ235 significantly increases dexamethasone activity in T-ALL models through increased apoptosis

(A) Representative flow cytometry plots demonstrating apoptosis in COG-LL-317h (top) and RS4;11 (bottom) treated with vehicle (0.01% dimethyl sulfoxide [DMSO]), BEZ235 (BEZ; 1μM), dexamethasone (DEX; 200 nM), or BEZ235 plus dexamethasone (BEZ+DEX; 1 μM and 200 nM respectively) for 36 hours. Cells were analyzed for phosphotidylserine expression on the outer surface by staining with an anti-Annexin V-FITC conjugated antibody and also the intercalating agent propidium iodide (PI). Cells in the lower right quadrants are the Annexin V-FITC positive and PI negative (defined as early apoptosis) and cells in the upper right quadrant represent the cells that are Annexin V-FITC positive and PI positive (defined as late apoptosis). **(B)** Mean values and standard deviations (error bars) of Annexin V-FITC positive cells (lower and upper right quadrants) are shown for triplicate samples assayed over two separate experiments for COG-LL-317h (left) and RS4;11 (right). **(C)** Western blot analysis examining caspase cleavage in COG-LL-317h following treatment with vehicle (0.01% DMSO), BEZ235 (BEZ; 1μM), dexamethasone (DEX; 200

nM), or the BEZ235 plus dexamethasone (BEZ+DEX; 1 μM and 200 nM respectively) for 36 hours.

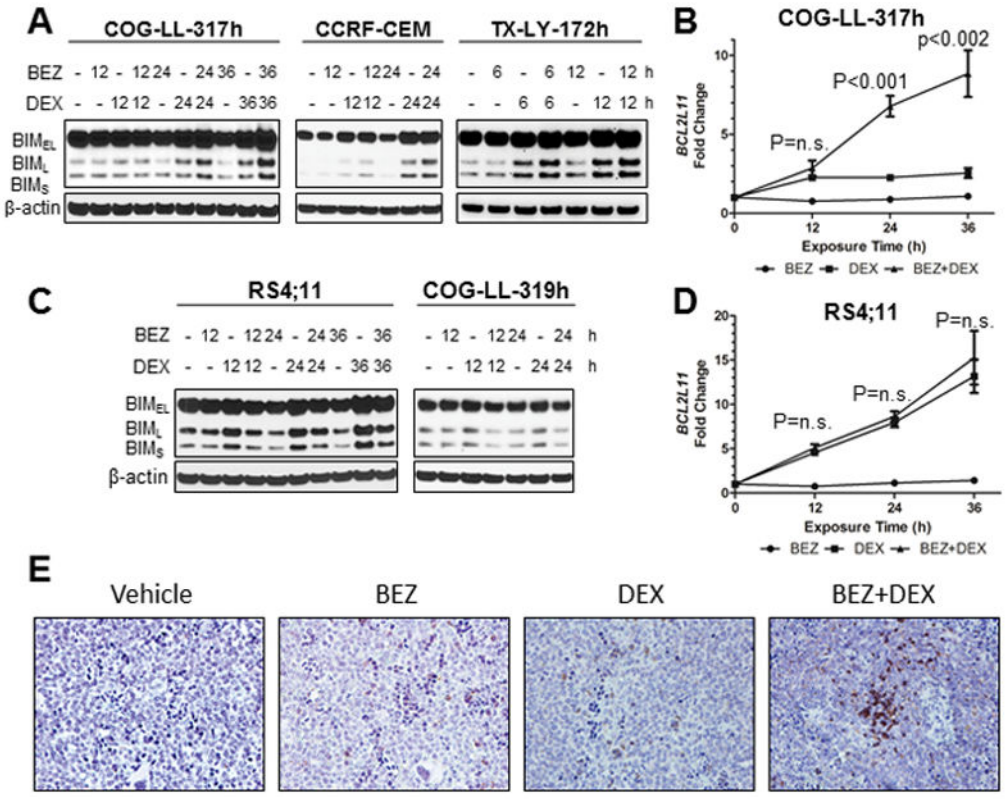

Figure 4. BEZ235 increases dexamethasone-induced expression of BIM

(A) Western blot analysis examining BIM_{EL}, BIM_L, and BIM_S expression in T-ALL models COG-LL-317h (left), CCRF-CEM (middle), and TX-LY-172h (right) after treatment with vehicle (0.01% DMSO), BEZ235 (BEZ; 1μM), dexamethasone (DEX; 200 nM), or the BEZ235 plus dexamethasone (BEZ+DEX; 1 μM and 200 nM respectively) for the indicated number of hours. **(B)** Quantitative RT-PCR analysis of *BCL2L11* transcripts in T-ALL model COG-LL-317h when treated with vehicle (0.01% DMSO), BEZ235 (BEZ; 1μM), dexamethasone (DEX; 200 nM), or the BEZ235 plus dexamethasone (BEZ+DEX; 1 μM and 200 nM respectively) for 12, 24, or 36 hours. **(C)** Western blot analysis examining BIM_{EL}, BIM_L, and BIM_S expression in B-ALL models RS4;11 (left) and COG-LL-319h (right) after treatment with vehicle (0.01% DMSO), BEZ235 (BEZ; 1μM), dexamethasone (DEX; 200 nM), or the BEZ235 plus dexamethasone (BEZ+DEX; 1 μM and 200 nM respectively) for the indicated number of hours. **(D)** Quantitative RT-PCR of *BCL2L11* transcripts in B-ALL model RS4;11 when treated with vehicle (0.01% DMSO), BEZ235 (BEZ; 1μM), dexamethasone (DEX; 200 nM), or the BEZ235 plus dexamethasone (BEZ+DEX; 1 μM and 200 nM respectively) for 12, 24, or 36 hours. **(E)** Immunohistochemistry staining for BIM in splenic tissue isolated from mice following 7 days of treatment with vehicle (NMP:PEG300 [1:9, v/v] via oral gavage + 5% glucose via intraperitoneal injection), BEZ235 (10 mg/kg via oral gavage), dexamethasone (7.5 mg/kg via intraperitoneal injection), or BEZ235 (10 mg/kg) + Dexamethasone (7.5 mg/kg). Brown indicates positive signal within tissue.

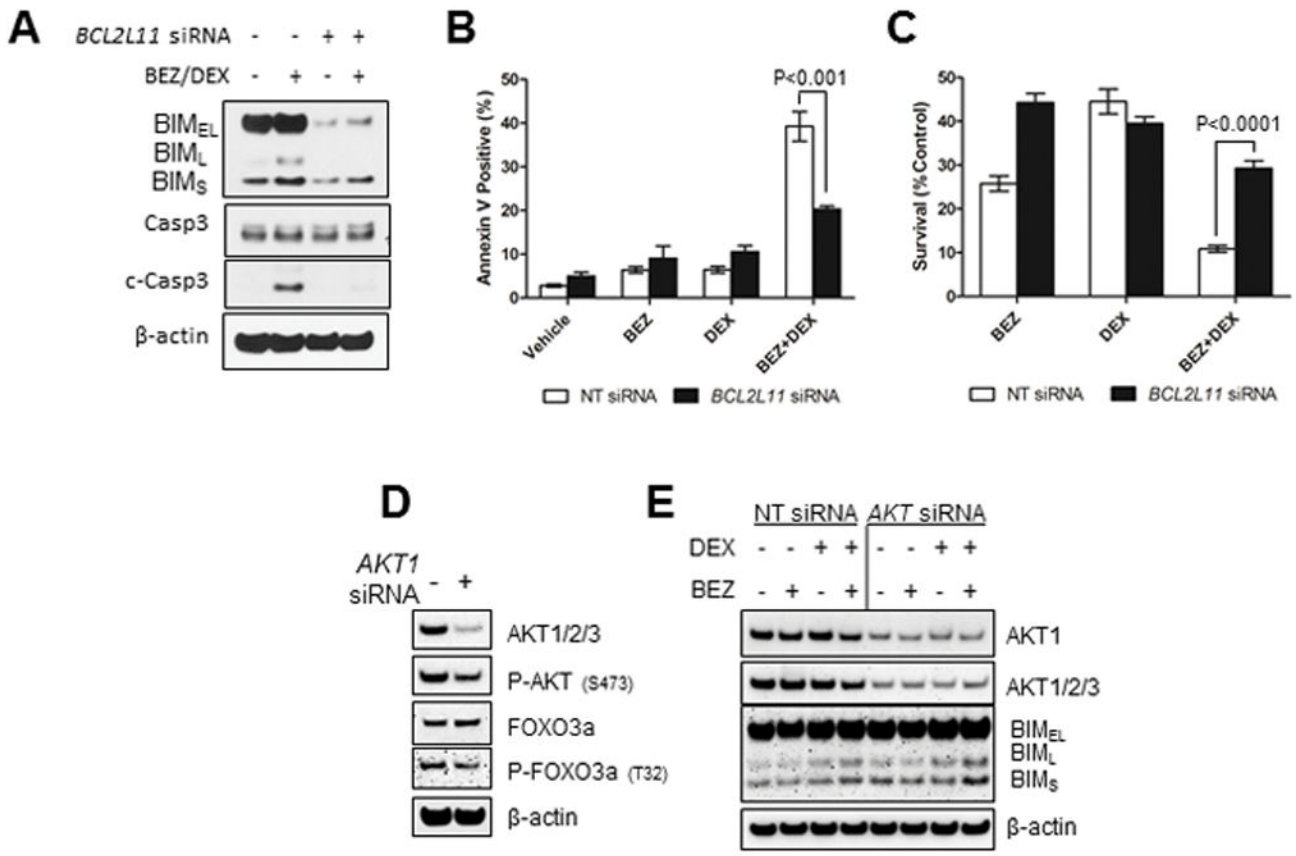

Figure 5. AKT1 contributes to dexamethasone-resistance by suppressing BIM

(A) Western blot analysis examining BIM expression and caspase cleavage in COG-LL-317h cells following transfection with non-targeting siRNA control or siRNA against *BCL2L11* and treatment for 36 hours with vehicle (0.01% DMSO) or BEZ235 plus dexamethasone (1μM and 200nM respectively). **(B)** Flow cytometry analysis examining apoptosis as measured by Annexin V positivity in COG-LL-317h cells following transfection with non-targeting siRNA control or siRNA against *BCL2L11* and treatment for 36 hours with vehicle (0.01% DMSO), BEZ235 (BEZ; 1μM), dexamethasone (DEX; 200 nM), or the BEZ235 plus dexamethasone (BEZ+DEX; 1 μM and 200 nM respectively). The mean values and standard deviations (error bars) of Annexin V-FITC positive cells are shown for triplicate samples assayed over two separate experiments. **(C)** Cytotoxicity as determined by DIMSCAN in COG-LL-317h cells following transfection with non-targeting siRNA control or siRNA against *BCL2L11* and treatment with vehicle (0.01% DMSO), BEZ235 (BEZ; 1μM), dexamethasone (DEX; 200 nM), or the BEZ235 plus dexamethasone (BEZ+DEX; 1 μM and 200 nM respectively). The mean values and standard deviations (error bars) relative to vehicle only treated cells are shown for 12 replicates. **(D)** Western blot analysis of COG-LL-317h cells transfected with non-targeting siRNA or siRNA against *AKT1* after incubation for 48 hours demonstrating sustained knockdown of AKT activity. **(E)** Western blot analysis examining BIM induction in COG-LL-317h cells following transfection with non-targeting siRNA control or siRNA against *AKT1* and treatment for 24

hours with vehicle (0.01% DMSO) BEZ235 (BEZ; 1uM), dexamethasone (DEX; 200nM), or BEZ235 plus dexamethasone (BEZ+DEX).

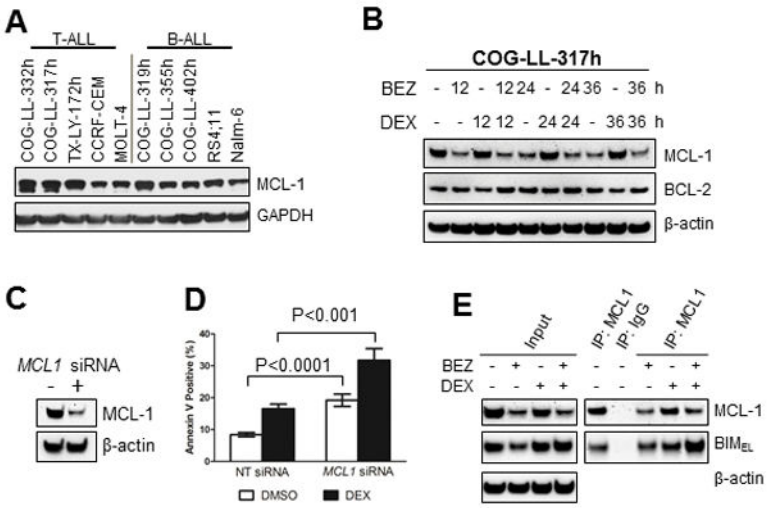

Figure 6. BEZ235 decreases MCL-1 suppression of BIM-induced apoptosis in COG-LL-317h

(A) Western blot analysis comparing basal expression of MCL-1 in T-ALL (left) and B-ALL (right) cell lines while in their log-phase of growth. **(B)** Western blot analysis examining MCL-1 and BCL-2 expression in T-ALL model COG-LL-317h after treatment with vehicle (0.01% DMSO), BEZ235 (BEZ; 1μM), dexamethasone (DEX; 200 nM), or the BEZ235 plus dexamethasone (BEZ+DEX; 1 μM and 200 nM respectively) for 12, 24, or 36 hours. **(C)** Western blot analysis examining MCL-1 expression in COG-LL-317h cells following transfection with non-targeting siRNA control or siRNA against *MCL1* and incubation for 48 hours. **(D)** Flow cytometry analysis examining apoptosis by measuring Annexin V positivity in COG-LL-317h cells following transfection with non-targeting siRNA control or siRNA against *MCL1* and treatment with or without dexamethasone (DEX; 200 nM). The mean values and standard deviations (error bars) of Annexin V-FITC positive cells are shown for triplicate samples assayed over two separate experiments. **(E)** Immunoprecipitation of MCL-1 with BIM in COG-LL-317h cells treated with vehicle (0.01% DMSO), BEZ235 (BEZ; 1uM), dexamethasone (DEX; 200nM), or BEZ235 plus dexamethasone (BEZ+DEX; 1uM and 200nM respectively). Protein lysates from COG-LL-317h cells treated with respective agents were exposed to MCL-1 or IgG antibody bound to Protein G. Resulting immunoprecipitate was blotted with antibodies against MCL-1 and BIM (right). Input lysate was blotted with antibodies against MCL-1 and BIM (left).